Thermally Evaporated Aerosol OT Thin Films as Templates for the Room Temperature Synthesis of Aragonite Crystals

Debabrata Rautaray, S. R. Sainkar, and Murali Sastry*

Materials Chemistry Division, National Chemical Laboratory, Pune 411 008, India

Received April 4, 2003. Revised Manuscript Received May 7, 2003

The growth of calcium carbonate crystals within thermally evaporated aerosol OT (AOT) thin films is described. In situ crystal growth is accomplished by a process of Ca^{2+} ion entrapment in the AOT host followed by CO_3^{2-} ion reaction. The $CaCO_3$ crystals exhibited almost 100% aragonite crystal structure and were in the form of bundles of aragonite needles. The fact that a similar ion exchange process in thermally evaporated stearic acid films resulted in growth of oriented calcite crystals underlines the role of the lipid matrix in determining the crystal structure of the nucleating phase. Contact angle measurements of the $CaCO_3$−AOT films indicated that they were hydrophobic, thus pointing to the possible role of hydrophobic interaction between the AOT monolayer-covered $CaCO_3$ crystals in the assembly process.

Introduction

By adapting biological principles, materials scientists are attempting to produce novel materials. Substantial progress has been made in understanding how biomineralization occurs and how to exploit the basic principles involved in it.[1] One of the requirements for biomineralization is epitaxy between the crystal nucleating face and the underlying bio-organic surface, and, consequently, biomimetic surfaces such as those presented by Langmuir monolayers,[2−4] self-assembled monolayers (SAMs),[5] and functionalized polymer surfaces[6] have been studied in great detail. Attempts have also been made to control the morphology of crystals via addition of suitable crystallization inhibitors[7] and carrying out crystal growth in constrained environments such as those afforded by microemulsions.[8] Insofar as growth of $CaCO_3$ crystals on biomimetic templates such as SAMs is concerned, Aizenberg, Black, and Whitesides have shown that lattice match at the interface is not always essential and that orientational match between carboxylate ions in SAMs and carbonate ions in the calcite nucleating phase is often more important.[5b] This leads to oriented growth of $CaCO_3$ crystals on surfaces such as terminally functionalized SAMs supported on metal films[5] and also on functionalized polymeric crystallization templates.[6c] Travaille et al. have shown interesting hexagonal organization of highly oriented calcite crystals on Au (111) films covered by a monolayer of 16-mercaptohexadecanoic acid.[5c] Very recently Donners et al.[6c] have demonstrated the use of a shape-persistent polymeric crystallization template [poly(L-isocyanoalanyl-D-alanine)] in the growth of calcite wherein crystal growth was influenced by both nucleation and adsorption processes.

Biominerals based on calcium carbonate are complicated by the formation of the three stable polymorphs calcite, aragonite, and vaterite.[9] Aragonite is known to have very high mechanical strength and is metastable under ambient conditions.[2] A classical example is that of nacre in which growth of platelike aragonite crystals occurs within a complex organic matrix.[2] In comparison, the laboratory synthesis of aragonite at room temperature has been very difficult to achieve without the use of soluble additives such as small organic molecules or Mg^{2+} ions[10a,b,c] but has been achieved at slightly elevated temperatures.[5a,10c,d] On the other hand, there are

* Author for correspondence. Phone: + 91 20 5893044. Fax: +91 20 5893952 or 5893044. E-mail: sastry@ems.ncl.res.in.

(1) Heuer, A. H.; Fink, D. J.; Laraia, V. J.; Arias, J. L.; Calvert, P. D.; Kendall, K.; Messing, G. L.; Blackwell, J.; Rieke, P. C.; Thomoson, D. H.; Wheeler, A. P.; Veis, A.; Caplan, A. I. *Science* **1992**, *255*, 1098.

(2) Litvin, A. L.; Valiyaveettil, S.; Kaplan, D. L.; Mann, S. *Adv. Mater.* **1997**, *9*, 124.

(3) Heywood, B. R.; Mann, S. *Adv. Mater.* **1994**, *6*, 9, and references therein.

(4) $BaSO_4$: (a) Heywood, B. R.; Mann, S. *Langmuir* **1992**, *8*, 1492. (b) Heywood, B. R.; Mann, S. *J. Am. Chem. Soc.* **1992**, *114*, 4681. (c) Buijnsters, P. J. J. A.; Donners, J. J. J. M.; Hill, S. J.; Heywood, B. R.; Nolte, R. J. M.; Zwanenburg, B.; Sommerdijk, N. A. J. M. *Langmuir* **2001**, *17*, 3623.

(5) $CaCO_3$/$SrCO_3$: (a) Kuther, J.; Nelles, G.; Seshadri, R.; Schaub, M.; Butt, H.-J.; Tremel, W. *Chem. Eur. J.* **1998**, *4*, 1834. $CaCO_3$: (b) Aizenberg, J.; Black, A. J.; Whitesides, G. M. *J. Am. Chem. Soc.* **1999**, *121*, 4500. (c) Travaille, A. M.; Donners, J. J. J. M.; Gerritsen, J. W.; Sommerdijk, N. A. J. M.; Nolte, R. J. M.; Kempen, H. V. *Adv. Mater.* **2002**, *14*, 492−495.

(6) (a) Feng, S.; Bein, T. *Science* **1994**, *265*, 1839. (b) Falini, G.; Gazzano, M.; Ripamonti, A. *Adv. Mater.* **1994**, *6*, 46. (c) Donners, J. J. J. M.; Nolte, R. J. M.; Sommerdijk, N. A. J. M. *J. Am. Chem. Soc.* **2002**, *124*, 9700−9701.

(7) $BaSO_4$: (a) Bromley, L. A.; Cottier, D.; Davey, R. J.; Dobbs, B.; Smith, S.; Heywood, B. R. *Langmuir* **1993**, *9*, 3594. (b) Qi, L.; Coffen, H.; Antonietti, M. *Angew. Chem., Intl. Ed.* **2000**, *39*, 604. (c) Uchida, M.; Sue, A.; Yoshioka, T.; Okuwaki, A. *CrystEngComm* **2001**, 5.

(8) (a) Hopwood, J. D.; Mann, S. *Chem. Mater.* **1997**, *9*, 950. (b) Li, M.; Mann, S. *Langmuir* **2000**, *16*, 7088. (c) Hopwood, J. D.; Mann, S. *Chem. Mater.* **1997**, *9*, 1819. (d) Summers, M.; Eastoe, J.; Davis, S. *Langmuir* **2002**, *18*, 5023−5026.

(9) McGrath K. M. *Adv. Mater.* **2001**, *13*, 989.

(10) (a) Sugawara, A.; Kato, T. *Chem. Commun.* **2000**, 487−488. (b) Walsh, D.; Mann, S. *Nature* **1995**, *377*, 320. (c) Ota, Y.; Inui, S.; Iwashita, T.; Kasuga, T.; Abe, Y. *J. Am. Ceram. Soc.* **1995**, *78*, 1983. (d) Kuther, J.; Tremel, W. *Chem. Commun.* **1997**, 2029−2030.

10.1021/cm0342344 CCC: $25.00
Published on Web 05/30/2003

very few reports of room-temperature synthesis of aragonite without additives. Litvin et al have shown the formation of aragonite crystals at the air−water interface using compressed monolayers of 5-hexadecyloxyisophthalic acid,[2] and Heywood et al have reported aragonite synthesis under monolayers of eicosanoic acid and *n*-eicosyl sulfate at the air−water interface.[11] Kuther and co-workers have also observed growth of aragonite needles at slightly elevated temperature (45 °C) on SAMs when the terminal functionality of the self-assembling molecule (anthracene terminated thiol, ANTH) was tailored to force assembly into a rectangular lattice.[5a]

In this laboratory, we have developed a process based on thermally evaporated ionizable lipid films for the electrostatic entrapment of inorganic ions,[12] surface-modified nanoparticles,[13] proteins/enzymes,[14,15] and DNA.[15] One interesting possibility is the growth of minerals within the bilayer stacks by suitable reaction of entrapped metal cations. We have recently reported on the growth of $BaSO_4$,[16a] $CaCO_3$,[16b] and $SrCO_3$[16c] crystals in thermally evaporated stearic acid thin films. The anionic surfactant sodium bis-2-ethylhexyl-sulfosuccinate (aerosol OT, AOT) is a twin-tailed surfactant and is most commonly used to make reverse micelles because of its bulky hydrophobic tail relative to the hydrophilic group. This anionic surfactant has been used in the synthesis of nanoparticles of barium chromate,[17] barium sulfate,[8b,c,d] calcium sulfate,[18] barium carbonate,[19] and silica[20] in microemulsions. In this report, we demonstrate the growth of calcium carbonate crystals in thermally evaporated aerosol OT films by an ion exchange process. We observe the growth of bundles of aragonite needles in this matrix at room temperature without the use of additives. This is to be contrasted with rhombohedral calcite crystals that grow in thermally evaporated stearic acid films[16b] thus underlining the crucial role of lipid matrix in determining not only the morphology of the minerals, but also its crystallography.

Experimental Details

Aerosol OT (99.93% pure), calcium chloride, and sodium carbonate were obtained from Aldrich Chemicals and used without purification.

Thin films of aerosol OT ($C_{20}H_{37}NaO_7S$, MW 444.56) of 500-Å thickness were thermally vacuum deposited,[21] in an Edwards E306 vacuum coating unit operated at a pressure of 1×10^{-7} Torr, onto gold-coated AT-cut quartz crystals (for monitoring film thickness), glass, and Si (111) substrates for measurement by X-ray diffraction (XRD), Fourier transform infrared (FTIR) spectroscopy, and scanning electron microscopy (SEM). The surfactant was deposited by a process of sublimation in a vacuum at a temperature not exceeding 80 °C for a period of 5 min. FTIR analysis of the thermally evaporated aerosol OT film showed no evidence of thermal degradation of the surfactant molecules. The film thickness was monitored using a QCM fitted to the deposition chamber and crosschecked by ellipsometry measurements.

After deposition, the AOT thin films on Si (111) and glass substrates were immersed in 50 mL of 10^{-2} M aqueous $CaCl_2$ solution (pH 6) for 4 h. The resulting Ca−sulfosuccinate films on Si (111) and glass substrates were washed with double-distilled water and dried under flowing nitrogen, and subjected to FTIR and XRD analysis, respectively. Thereafter, growth of calcium carbonate in the Ca−AOT thin films was achieved by immersion of these films in 50 mL of 2.4×10^{-3} M Na_2CO_3 aqueous solution (pH 6) for 3 h. The $CaCO_3$ crystals grown within 500-Å thick AOT films were washed with double-distilled water, dried under flowing nitrogen, and subjected to FTIR measurements carried out in the diffuse transmittance mode at a resolution of 4 cm^{-1} on a Shimadzu FTIR-8201 PC instrument.

X-ray diffraction (XRD) measurements of the Ca−sulfosuccinate and $CaCO_3$−AOT films on glass were carried out in the transmission mode on a Philips PW 1830 instrument operating at 40 kV voltage and a current of 30 mA with Cu Kα radiation. Scanning electron microscopy (SEM) measurements of the $CaCO_3$−AOT films on Si (111) substrates were carried out on a Leica Stereoscan-440 instrument equipped with a Phoenix energy dispersive analysis of X-rays (EDAX) attachment. Prior to XRD and SEM studies, these films were subjected to mild ultrasonic agitation in water for ca. 3 min to dislodge any $CaCO_3$ crystals that had nucleated in the solution and had bound weakly to the AOT film surface.

To determine whether the growth of these crystals was purely a surface process, contact angles were measured at various points on the films. Contact angle measurements were carried out on a 1-μL sessile water drop using a Rame-Hart 100 goniometer on at least 10 different points on the film surface.

To better understand the role of the AOT thin film in polymorph selectivity and morphology control of $CaCO_3$ crystals, the kinetics of crystallization was monitored in the following manner. Thin films of AOT of 500-Å thickness were deposited on Si (111) and glass substrates and immersed in aqueous $CaCl_2$ solution under the experimental conditions mentioned above. After entrapment of Ca^{2+} ions, the calcium−sulfosuccinate film was immersed in Na_2CO_3 solution and the crystallization of $CaCO_3$ was monitored by SEM and XRD and reported as a function of time of immersion.

Results and Discussion

The first step in our study was determining whether the sodium ions in aerosol OT are completely replaced by Ca^{2+} ions during immersion in $CaCl_2$ solution. A chemical analysis of the as-deposited 500-Å thick AOT film on a Si (111) substrate before and after immersion in $CaCl_2$ solution for 3 h was done using EDAX (Figure 1, curves 1 and 2, respectively). It is shown that the as-deposited AOT thin film shows the presence of Na, S, C, and O signals (curve 1). A quantitative analysis of the Na and S components yielded a 1:1.1 atomic ratio for Na/S, in excellent agreement with the expected stoichiometry. After immersion of the AOT film in $CaCl_2$ solution, the Na signal completely disappeared (curve 2) and a strong Ca signal appeared. Within the detection limits of the EDAX instrument, this result indicates

(11) Heywood, B. R.; Mann, S. *Chem. Mater.* **1994**, *6*, 311−318.
(12) Ganguly, P.; Sastry, M.; Pal, S.; Shashikala, M. N. *Langmuir* **1995**, *11*, 1078.
(13) Patil, V.; Malvankar, R. B.; Sastry, M. *Langmuir* **1999**, *15*, 8197.
(14) Gole, A.; Vyas, S.; Sainkar, S. R.; Lachke, A.; Sastry, M. *Langmuir* **2001**, 17, 5964.
(15) Ramakrishnan, V.; Sable, M.; D'Costa, M.; Ganesh, K. N.; Sastry, M. *Chem. Commun.* **2001**, 2622.
(16) (a) Rautaray, D.; Kumar, A.; Reddy, S.; Sainkar, S. R.; Sastry, M. *Cryst. Growth Des.* **2002**, *2*, 197. (b) Damle, C.; Kumar, A.; Bhagwat, M.; Sainkar, S. R.; Sastry, M. *Langmuir* **2002**, *18*, 6075. (c) Sastry, M.; Kumar, A.; Damle, C.; Sainkar, S. R.; Bhagwat, M.; Ramaswami, V. *CrystEngComm* **2001**, 21.
(17) Li, M.; Schnablegger, H.; Mann, S. *Nature* **1999**, *402*, 393.
(18) Rees, G. D.; Evans-Gowing, R.; Hammond, S. J.; Robinson, B. H. *Langmuir* **1999**, *15*, 1993.
(19) Qi, L.; Ma, J.; Cheng, H.; Zhao, Z. *J. Phys. Chem. B* **1997**, *101*, 3460.
(20) Arriagada, F. J.; Osseo-Asare, K. *J. Colloid Interface Sci.* **1995**, *170*, 8.
(21) Ganguly, P.; Pal, S.; Sastry, M.; Shashikala, M. N. *Langmuir* **1995**, *11*, 1078−1080.

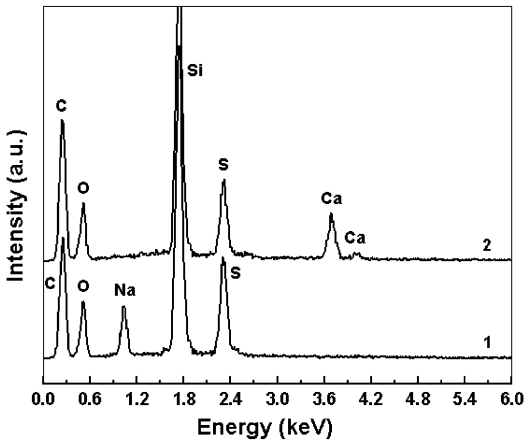

Figure 1. EDAX spectra recorded from a 500-Å-thick aerosol OT thin film on a Si (111) substrate (curve 1) and the aerosol OT film after incorporation of Ca^{2+} ions (curve 2).

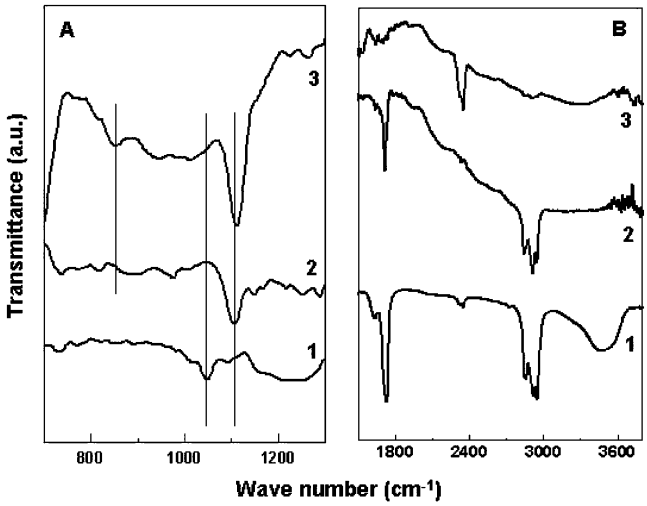

Figure 2. (A and B) FTIR spectra recorded from a 500-Å-thick aerosol OT film on a Si (111) substrate (curve 1), the aerosol OT film after incorporation of Ca^{2+} ions (curve 2), and the calcium sulfosuccinate film after incorporation of CO_3^{2-} ions (curve 3) in different spectral regions.

complete replacement of the Na^+ ions by Ca^{2+} ions in the AOT thin film. A quantitative analysis of the Ca and S components yielded a 1:1.86 atomic ratio for Ca/S. This is in excellent agreement with the expected Ca/S ratio of 1:2 based on charge neutrality considerations. Thus, the EDAX analysis indicates that the 3-h immersion time for AOT in the $CaCl_2$ solution is optimum for formation of Ca−AOT.

Figure 2 shows the FTIR spectra recorded from the as-deposited 500-Å thick aerosol OT film on a Si (111) substrate (curve 1), the aerosol OT film after entrapment of Ca^{2+} ions (curve 2), and the calcium sulfosuccinate film after reaction with Na_2CO_3 (curve 3). Prominent absorption bands are seen at 1057 (Figure 2A, curve 1), 1700, 2850, and 2920 cm^{-1} (Figure 2B, curve 1) in the case of the as-deposited aerosol OT film. The band at 1057 cm^{-1} is assigned to the S═O stretching vibration of the sulfonate group present in the AOT molecules.[22] The band at 1700 cm^{-1} is due to carbonyl stretch vibrations in the AOT molecules, and the two bands at 2850 and 2920 cm^{-1} have been assigned to the methylene symmetric and antisymmetric stretching vibrations, respectively, in the hydrocarbon chains (Figure 2B, curve 1). After entrapment of Ca^{2+} ions in the AOT thin film, the absorption band at 1057 cm^{-1} has shifted to 1113 cm^{-1} (Figure 2A, curve 2) clearly indicating that the Ca^{2+} ions have complexed electrostatically with the sulfonate groups in the film. The methylene antisymmetric and symmetric vibrations have reduced marginally in intensity following Ca^{2+} incorporation (Figure 2B, curve 2). The FTIR spectrum recorded from the calcium sulfosuccinate film after reaction with Na_2CO_3 (curve 3) shows the presence of absorption bands at 1113 and 855 cm^{-1}. Retention of the 1113 cm^{-1} band after Na_2CO_3 treatment indicates that not all of the Ca^{2+} ions have reacted with carbonate ions to form calcium carbonate. The feature centered at 855 cm^{-1} is characteristic of the aragonite polymorph[23] and shows unequivocally the formation of these crystals in the AOT matrix. There is no evidence of either calcite or vaterite polymorphs of $CaCO_3$ which are known to show strong infrared absorption bands at 712, 874, and 744 cm^{-1}, and 877 cm^{-1} respectively.[23] The almost complete disappearance of the methylene antisymmetric and symmetric vibration bands after aragonite formation (curve 3, Figure 2B) indicates considerable reorganization in the film, possibly due to randomization of AOT hydrocarbon chain orientation around the aragonite crystals.

As briefly mentioned in the Introduction, it has been shown in this laboratory that immersion of thermally evaporated fatty acid films into electrolyte solutions such as $PbCl_2$ and $CdCl_2$ resulted in the electrostatic entrapment of the metal cations and the spontaneous ordering of the lipid films into a lamellar *c*-axis oriented structure.[12] We have used this approach to form calcium sulfosuccinate films by immersion of 500-Å-thick AOT films in $CaCl_2$ solution. The formation of lamellar calcium sulfosuccinate was ascertained by the presence of characteristic odd−even intensity oscillations in the (00l) Bragg reflections in the XRD pattern of the film[12] (Figure 3, inset). These Bragg reflections are not observed in as-deposited AOT films (Supporting Information, S1A, curve 0 min.). From the periodicity of the (00l) Bragg reflections, the thickness of the calcium sulfosuccinate bilayers is calculated to be 48 Å and is consistent with the AOT molecular size of ∼ 22 Å. The *c*-axis oriented lamellar structure of a calcium sulfosuccinate bilayer is illustrated in the Figure 4A. For simplicity, only one bilayer of calcium sulfosuccinate resting on a monolayer of AOT in contact with the substrate is shown in the schematic (Figure 4A). In reality, a 500-Å-thick calcium sulfosuccinate film would consist of roughly 10 such bilayers stacked one on top of the other.

SEM pictures recorded from a 500-Å-thick Ca−AOT film on a Si (111) substrate after immersion in Na_2CO_3 solution for 160 min are shown in Figure 4B and C at different magnifications. The low magnification image

(22) Silverstein, R. M.; Webster, F. X. *Spectrometric Identification of Organic Compounds,* 6th ed.; John Wiley & Sons: New York, 1998; p 107.

(23) (a) Nassrallah-Aboukais, N.; Boughriet, A.; Laureyns, J.; Aboukais, A.; Fischer, J. C.; Langelin, H. R.; Wartel, M. *Chem. Mater.* **1998**, *10*, 238−243. (b) Falini, G.; Albeck, S.; Weiner, S.; Addadi, L. *Science* **1996**, *271*, 67−69.

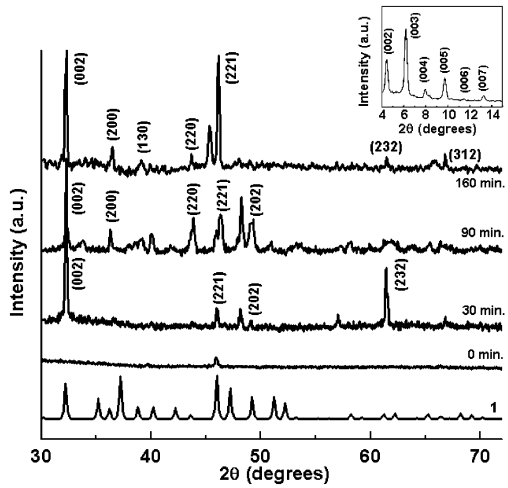

Figure 3. Simulated powder XRD pattern of aragonite crystals (Curve 1). XRD pattern recorded from $CaCO_3$ crystals grown within a 500-Å-thick thermally evaporated AOT film at different time intervals of crystal growth. The inset shows the XRD pattern recorded from a 500-Å- thick AOT film after entrapment of Ca^{2+} ions. The (00l) Bragg reflections are indexed in this figure.

(Figure 4B) shows densely populated, well-organized bundles of $CaCO_3$ needles. EDAX analysis of the $CaCO_3$ needles yielded a Ca/C/O atomic ratio of 1:1.3:8. Although the Ca/C ratio is in fair agreement with the expected stoichiometry, excess oxygen is due to sampling from the silica substrate. The XRD patterns recorded from the $CaCO_3$ crystals shown in Figure 4B and C are shown in Figure 3, the curve identified by the appropriate time of reaction. A number of Bragg reflections are identified and have been indexed with reference to the unit cell of the aragonite structure (a = 4.959 Å, b = 7.968 Å, c = 5.741 Å; space group *Pmcn*).[10c,24] For comparison, the simulated powder XRD pattern of aragonite is shown as curve 1 in Figure 3. That there was no evidence of either calcite or vaterite formation in the thermally evaporated AOT film is a salient feature of this investigation. The XRD data thus provide clear support for the morphology of the $CaCO_3$ crystals seen in the SEM images − such well-defined needles are known to be characteristic of the aragonite polymorph.[5a,10c] Additionally, the presence of intense (002), (200), and (221) reflections indicates oriented growth of the aragonite needles along these crystallographic planes. The higher-magnification SEM image (Figure 4C) recorded from the $CaCO_3$−AOT film clearly shows smaller, individual bundles of aragonite crystals with the needles nucleating from a central crystallite which was in contact with the organic surface. It is pertinent to mention here that previous reports on aragonite crystallization have been carried out in the presence of soluble additives such as Mg^{2+} ions,[10a−c] and at elevated temperature,[5a,10c,d] with the exception of the reports of Litvin et al.[2] and Heywood et al.[11] as briefly discussed in the Introduction. In this study, we have been able to achieve phase-pure aragonite growth at room temperature with AOT as a crystallization template.

(24) The XRD patterns were indexed with reference to the unit cell of the aragonite structure from ASTM chart card no. 5-0453 (a = 4.959 Å, b = 7.968 Å, c = 5.741 Å; space group *Pmcn*).

It is possible that the growth of the aragonite crystals occurs in solution by a process of leaching out of Ca^{2+} ions from the calcium−sulfosuccinate film followed by reaction with carbonate ions and attachment of the crystals thus formed to the surface of the AOT film. This possibility must be discounted before in situ growth of the aragonite crystals within the AOT matrix can be accepted as a plausible mechanism. One possible method to ascertain the mechanism is to monitor the growth of the aragonite crystals as a function of time of immersion in the Na_2CO_3 solution. SEM pictures recorded from a 500-Å-thick calcium−sulfosuccinate film on a Si (111) wafer after immersion in Na_2CO_3 solution for 30, 60, 90, 120, and 160 min are shown in Figures 5A−E, respectively. After 30 min of reaction, the SEM image (Figure 5A) shows the growth of very small $CaCO_3$ crystals apparently within the AOT film. After a further 30 min of reaction, the growth of smaller individual bundles of aragonite crystals is observed (Figure 5B). Reaction of the calcium−sulfosuccinate film for 90 min leads to the formation of bigger but immature bundles of aragonite crystals (Figure 5C). Immersion of the calcium−sulfosuccinate film for a further 30 min in the Na_2CO_3 solution resulted in bundles of aragonite needles branching out from a central point that was in contact with the organic surface (Figure 5D). Reaction of the calcium−sulfosuccinate film for 160 min clearly shows assembly of individual bundles of aragonite crystals into a highly dense structure (Figure 5E). Although the morphology of the aragonite crystals in Figure 5D and E is not very different, the extent of assembly of the aragonite bundles appears to proceed with time and reach saturation after 160 min of reaction. Contact angle measurements carried out at each one of the reaction times in the SEM study yielded values in excess of 95° indicating that the film surface continued to be hydrophobic during formation of the aragonite crystals. Thus, the SEM images and contact angle measurements obtained from the calcium−sulfosuccinate film during growth of the aragonite crystals suggest that the growth process occurs within the AOT matrix and not externally by a leaching process.

The small and wide angle XRD patterns recorded from a 500-Å-thick AOT film on a glass substrate after immersion in $CaCl_2$ solution for 45, 90, 150, and 210 min are shown in the Supporting Information S1.A and B, respectively. The curve labeled 0 min in S1.A corresponds to the small angle XRD pattern recorded from the as-deposited AOT thin film. Bragg reflections are not observed in the as-deposited AOT film. As a function of time of immersion of the as-deposited AOT film in $CaCl_2$ solution, it is observed that the (00l) Bragg reflections slowly grow in intensity and reach saturation within 210 min of reaction. This clearly indicates evolution of lamellar order in the AOT film as the Ca^{2+} ions diffuse into the lipid matrix. Formation of lamellar calcium sulfosuccinate was ascertained by the presence of characteristic odd−even intensity oscillations in the (00l) Bragg reflections in the XRD pattern of the film (S1A, 210 min curve). Bragg reflections are absent in the wide angle XRD patterns shown in S1.B for all times of immersion of the AOT film in $CaCl_2$ solution. Therefore, in-plane ordering of the AOT molecules could not be detected by wide angle XRD measurements. How-

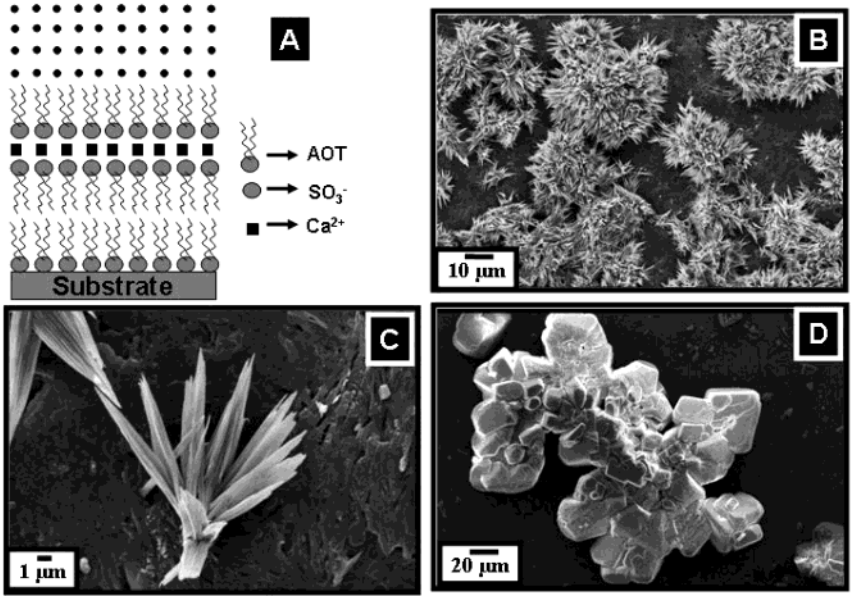

Figure 4. (A) Cartoon showing the expected lamellar structure of the thermally evaporated aerosol OT film after entrapment of Ca^{2+} counterions. (B and C) Representative SEM images of $CaCO_3$ crystals formed within a 500-Å-thick thermally evaporated aerosol OT film at different magnifications. (D) SEM image of $CaCO_3$ crystals formed within a 500-Å-thick thermally evaporated stearic acid film.

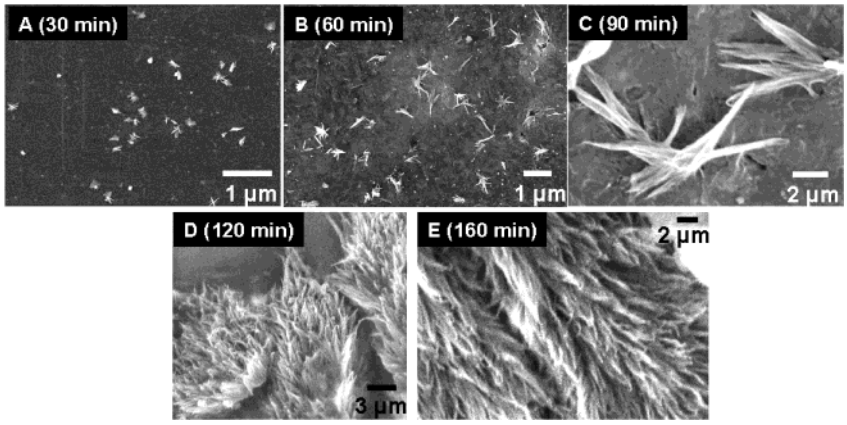

Figure 5. (A−E) Representative SEM images of $CaCO_3$ crystals grown in a 500-Å-thick thermally evaporated aerosol OT film at different time intervals of reaction of the precursor calcium−sulfosuccinate film with the CO_3^{2-} ions.

ever, this does not rule out the possibility of short range ordering of the AOT molecules in the thermally evaporated thin films which would be sufficient, in principle, to induce oriented growth of nuclei of aragonite.

The evolution of XRD patterns recorded as a function of time of reaction of Ca−AOT with carbonate ions is shown in Figure 3 and correspond to the SEM images shown in Figure 5A−E. A number of Bragg reflections are identified and have been indexed with reference to the unit cell of the aragonite structure.[10c,24] As expected, the Ca−AOT film before initiation of reaction shows no Bragg reflections in the region of interest (Figure 3, 0 min curve). As $CaCO_3$ growth proceeds, the Bragg reflections characteristic of aragonite grow in intensity and reach saturation after 160 min of reaction. It is observed that at the initial growth stage (30 min of reaction), the aragonite crystals show preferred orientation along the (002) direction. We have observed in the SEM images that further reaction leads to considerable assembly of the aragonite bundles (Figure 5C−E) and the possibility of reorientation of the crystallites. However, we observe that the (002) Bragg reflection remains the most intense even after 160 min of reaction. This indicates that the aragonite needle assembly proceeds without significant reorientation of the crystallites.

Our previous report on the crystallization of $CaCO_3$ within thermally evaporated stearic acid films resulted in the formation of highly oriented calcite crystals with a small percentage of the vaterite polymorph.[16b] In the study using stearic acid as the template, we did not observe the growth of the aragonite phase.[16b] Figure 4D shows an SEM image of $CaCO_3$ crystals grown within a 500-Å-thick stearic acid film under conditions identical to those adopted for AOT studies (see ref 16b for experimental details), wherein oriented growth of rhombohedral calcite crystals (at pH 6) can clearly be seen. It is clear from this study and our earlier work that the lipid matrix that acts as the host for crystal growth plays a significant role in determining not only the morphology of the minerals, but also its crystallography. Epitaxy between the nucleating crystal face and underlying template would determine the crystallography of the mineral and it is likely that the spatial arrangement of stearic acid and AOT molecules within the thermally

evaporated bilayers is significantly different. This is not difficult to understand given that the sizes of the carboxylic acid and sulfonate headgroups in stearic acid and AOT molecules, respectively, are very different. Although the exact packing of the AOT and stearic acid molecules in the thermally evaporated bilayer stacks is not known, we expect that it may not be significantly different for Langmuir monolayers or SAMs bearing similar polar functional groups. Litvin et al have reported that aragonite needle growth occurs under Langmuir monolayers of 5-hexadecyloxyisophthalic acid where each molecule resides in a rectangular lattice and interacts with two neighbors through hydrogen bonding.[2] Kuther and co-workers also observed growth of aragonite needles on SAMs when the terminal functionality of the self-assembling molecule (anthracene terminated thiol, ANTH) was changed to force assembly into a rectangular lattice.[5a] $CaCO_3$ crystals grown on otherwise hexagonally packed SAMs yielded calcite crystals.[8b] We believe that the bulky nature of the AOT headgroup forces it to pack in a rectangular pattern in thermally evaporated films, whereas stearic acid with smaller carboxylic acid headgroups would pack hexagonally. This would satisfactorily explain the difference in crystallography observed for $CaCO_3$ grown in the different templates. In a similar study, the fact that AOT possesses such organizational capability has been shown by Mann and co-workers in their study of the formation of linear chains, rectangular super lattices, and long filaments of $BaCrO_4$ crystals grown using AOT reverse micelle.[17] We emphasize that more work is required to fully substantiate this conclusion.

The formation of large bundles of aragonite needles is another interesting feature of this study. During initial stages of growth of the crystals, the AOT bilayers would distort to accommodate the large structures and eventually rupture to form a monolayer around the crystals. To determine whether the growth of these crystals was purely a surface process, we measured the contact angle at various points on the film surface at various stages of reaction and found that the surface was quite hydrophobic at all stages of reaction. The contact angles were measured on at least 10 different points on the film surface. The mean contact angle of the as-deposited AOT film was observed to be 95°. The mean contact angle of the calcium−sulfosuccinate film was 92°. The contact angles after the formation of the $CaCO_3$ crystals did not show any drastic change (mean contact angle of a water droplet 92°). During immersion in electrolyte solution and reaction with carbonate ions, the bilayers swell, and therefore, the nucleation of $CaCO_3$ occurs within this nano-container. Even though the crystals eventually grow to micron sizes (due to the flexibility of the lipid bilayers), the initial nucleation and growth stage is expected to be dominated by the nanodimensions of the cavity, and indeed, we observe interesting phase-selective nucleation of the crystals. No discernible loss of AOT from the film was observed during reaction of the Ca−AOT film with carbonate ions as detected by contact angle measurements carried out on the solution of immersion. The contact angle measurement result clearly shows that the aragonite needles of Figure 4B and C are covered with a monolayer of AOT, which renders them hydrophobic. The likely mechanism is therefore nucleation and growth of the aragonite crystals within the hydrophilic regions of the bilayers in the calcium−sulfosuccinate film accompanied by expansion of the lipid matrix (and consequent surface coating) to accommodate the large crystals. The hydrophobic nature of the crystallites points to a possible reason for formation of needlelike aragonite. Because the growth of the crystals occurs in an aqueous environment, hydrophobic forces between the AOT-monolayer-covered $CaCO_3$ crystals (at least in the very early stages of crystal growth) could lead to aggregation of the crystals into bundles of needlelike structures as observed.

In conclusion, the crystallization of calcium carbonate within thermally evaporated AOT films by a process of Ca^{2+} ion entrapment and thereafter reaction with CO_3^{2-} ions has been demonstrated. Under conditions where there is good registry between the Ca^{2+} ions and the underlying AOT template, oriented growth of predominantly aragonite crystals is observed at room temperature. The crystallography of $CaCO_3$ crystals is strongly dependent on the nature of the lipid in the thermally evaporated matrix and may be utilized to grow large quantities of minerals of well-controlled morphology and crystallography on different surfaces. Patterned lipid structures are also possible and add to the versatility of the technique.

Acknowledgment. D.R. thanks the Department of Science and Technology (DST), Government of India for financial assistance. This work was partially funded by grants to M.S. from the DST and the Indo-French Centre for the Promotion of Advanced Scientific Research (IFCPAR, New Delhi) and is gratefully acknowledged.

Supporting Information Available: Small and wide angle XRD patterns recorded from a 500-Å-thick AOT film after different times of reaction of calcium ions with the AOT thin film (S1.A) and the Ca−AOT film as a function of time of reaction with carbonate ions (S1.B) (PDF). This material is available free of charge via the Internet at http://pubs.acs.org.

CM0342344